The MROI fast tip-tilt correction and target acquisition system

John Young[a], David Buscher[a], Martin Fisher[a], Christopher Haniff[a], Alexander Rea[a], Eugene Seneta[a], Xiaowei Sun[a], Donald Wilson[a], Allen Farris[b], Andres Olivares[b] and Robert Selina[b]

[a] Cavendish Laboratory, University of Cambridge, JJ Thomson Avenue, Cambridge CB3 0HE, UK;

[b] Magdalena Ridge Observatory, New Mexico Institute of Mining and Technology, 801 Leroy Place, Socorro, NM, 87801

ABSTRACT

The fast tip-tilt correction system for the Magdalena Ridge Observatory Interferometer (MROI) is being designed and fabricated by the University of Cambridge. The design of the system is currently at an advanced stage and the performance of its critical subsystems has been verified in the laboratory. The system has been designed to meet a demanding set of specifications including satisfying all performance requirements in ambient temperatures down to -5 °C, maintaining the stability of the tip-tilt fiducial over a 5 °C temperature change without recourse to an optical reference, and a target acquisition mode with a $60''$ field-of-view. We describe the important technical features of the system, which uses an Andor electron-multiplying CCD camera protected by a thermal enclosure, a transmissive optical system with mounts incorporating passive thermal compensation, and custom control software running under Xenomai real-time Linux. We also report results from laboratory tests that demonstrate (a) the high stability of the custom optic mounts and (b) the low readout and compute latencies that will allow us to achieve a 40 Hz closed-loop bandwidth on bright targets.

Keywords: interferometry, tip-tilt correction

1. INTRODUCTION

The fast tip-tilt correction system for the Magdalena Ridge Observatory Interferometer[1] is being designed and built by the optical interferometry group at the Cavendish Laboratory of the University of Cambridge. Each system will perform closed-loop correction of atmospheric tip-tilt (angle of arrival) fluctuations on the light collected by an MROI Unit Telescope (UT), and will also function as a narrow-field target acquisition sensor. The preliminary design of the system has recently been completed; as part of this effort several key aspects of the design have been prototyped.

Reflecting its dual role, the official name for the system is the MROI Fast Tip-Tilt correction and Narrow-field Acquisition System (FTT/NAS). The interferometer system design[2] places an FTT/NAS on the Nasmyth optical table at each Unit Telescope (UT), where it is fed with light in the 350–1000 nm waveband reflected from a dichroic mirror. Other colours pass through the dichroic and are relayed to the beam combining laboratory.

The purpose of the FTT/NAS is to sense the location of an image of a celestial target with respect to a pre-determined fiducial point (referred to here as the tip-tilt zero point), and initially to send pointing corrections to the UT mount in order to move the target close to the zero point, and subsequently to detect and eliminate the smaller, rapidly varying tilt errors principally arising from atmospheric turbulence. This fast tip-tilt correction is accomplished by applying correction signals to a fast steering mirror (the UT secondary) and slowly-varying offloads to the telescope mount.

At the MROI, the location of the zero point will be realised each night, prior to observing, by sending co-aligned and parallel light beams simultaneously to the interferometric instruments and to the UTs. The instruments in the beam combining laboratory will be aligned with respect to the inward-propagating beams, while at each UT the relevant outward propagating beam will be directed onto the FTT/NAS sensor after back-reflection from the FTT/NAS dichroic, retro-reflection off a corner-cube installed on the UT Nasmyth table and subsequent transmission through the FTT/NAS dichroic.

Time-variable offsets may be applied to the zero point determined at the start of the night, in order to compensate for differential atmospheric refraction between the FTT sensor waveband and the fringe detection waveband, and/or to accommodate an off-axis tip-tilt reference object.

1.1 Top-level requirements

The following brief list summarises some of the most critical of the FTT/NAS requirements:

- Management of time varying offsets due to atmospheric dispersion and/or off-axis guiding;
- Supporting the streaming of "live" diagnostic telemetry;
- Supporting both acquisition and fast-guiding modes;
- Realising the sensitivity ($m_V = 16$ for a red target in $0.7''$ seeing) desired for faint-source science;
- Realising the zero-point stability requirements, especially in an exposed variable-temperature environment;
- Meeting the thermal dissipation budget;
- Designing a system that is compatible with the space constraints present on the Nasmyth optical table.

All of these requirements, and others not mentioned here, have influenced the design of the FTT/NA system. Although none of these requirements is individually unique, the combination has led to a design with some noteworthy features.

In the remainder of this paper we present our design, and describe how the requirements have driven it (Sec. 2). The methods and results of the laboratory validation carried out thus far are presented in Sec. 3. We then present our conclusions in Sec. 4, along with a brief summary of the development and integration tasks planned for the coming months.

2. DESIGN DESCRIPTION

Our design for the FTT/NA system is based around an off-the-shelf back-illuminated electron-multiplying CCD camera (Andor iXon X3 897), which offers fast readout, high quantum efficiency and sub-electron effective read noise, all of which are needed to meet the stringent closed-loop bandwidth and limiting magnitude requirements. Images from the FTT/NAS sensor will be interrogated by a local computer which will serve to both archive the data (either locally or via the central Interferometer Supervisory System (ISS)) and to send control demands to a fast steering mirror (the UT secondary mirror is used for this purpose, and will be supplied, complete with servo controller, by the UT vendor AMOS according to an MROI specification). Information on the current state of the UT mount, and any ancillary information needed by the FTT/NAS will be delivered via the ISS.

The Andor iXon X3 897 EMCCD camera is able to meet all our derived requirements associated with format, cost, cabling, mechanical stability, and heat dissipation. However, a custom readout mode will be needed to achieve the high frame rate and low latency required to deliver a 40 Hz closed-loop 3 dB bandwidth on bright targets. A preliminary 23×23 pixel custom mode has been implemented by Andor and tested in Cambridge. A 32×32 pixel derivative of this mode is now being developed by Andor, and offers the advantages of lower pattern noise due to clock-induced charge, and a larger field of view to accommodate field rotation when using an off-axis tip-tilt reference star.

We have chosen to use the same sensor for both target acquisition and fast tip-tilt correction, with a fixed pixel scale. A sufficiently large-format camera (at least 500×500 pixels), with suitable choice of image scale, allows both accurate image centroiding and a 60×60 arc second field-of-view for routine target acquisition.

The Andor EMCCD (as well as the alternative EMCCD cameras considered) is only guaranteed to operate effectively at a temperature above 0 °C and in a non-condensing environment, and so the FTT/NAS camera will be enclosed and a thermal control system supplied to maintain the temperature and humidity inside the camera enclosure at all times.

A critical design goal for the FTT/NAS is the need to ensure that its optics, together with the dichroic and the sensor camera must remain sufficiently stable in tilt and displacement such that the tip-tilt zero point (guiding centre) does not move by more than roughly half a micron on the detector surface over a night's observations*.

*The exact requirement is a variation of no more than 0.015 seconds of arc on the sky for a temperature change of 5 °C.

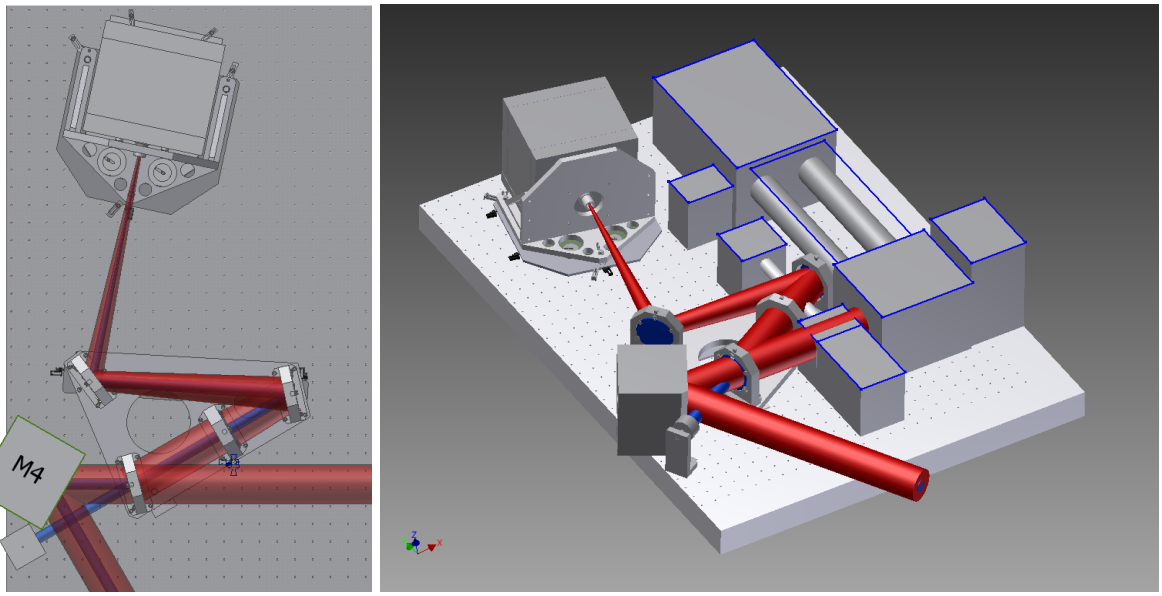

Figure 1. Left: A schematic diagram outlining the geometry of the FTT/NAS opto-mechanical layout. The beam from the UT tertiary mirror enters from bottom right and is intercepted by the dichroic to the right of the M4 mirror. The reflected beam passes through an apochromatic lens, and is focused onto the FTT/NAS camera sensor (at top) after reflection off two fold mirrors. Right: 3-d rendering of the FTT/NAS as it will be installed on the Nasmyth optical table. The featureless boxes represent the current space envelopes allocated to other hardware systems that will need to be located on the Nasmyth table.

To meet such high stability requirements we have chosen the perhaps unusual approach of employing mounts without adjusters for the optical components. This in turn will require the system to be tolerant of focus changes so that focus adjustment is only required seasonally. These stability requirements demand low sensitivity to thermal changes and so thermal gradients across the component mounts must be minimised. This has led us to adopt aluminium rather than stainless steel or invar (which performed only slightly better than aluminium due to its poor thermal conductivity, hence the additional material and fabrication costs were not warranted) for the mount material.

Our design envisions the fast tip-tilt loop being closed in software rather than with additional hardware, e.g. reconfigurable electronics such as FPGAs. This approach minimises the system's electrical power consumption. Basing our system on a standard PC has also allowed us to make the most extensive possible use of software libraries provided by the camera vendor.

A fixed frame rate of 1 kHz will be used for all but the faintest targets (there is no noise penalty for this due to the on-chip amplification) but the closed-loop bandwidth will be user-selectable by means of adjustable servo parameters that allow the degree of time-averaging of the correction signal to be altered by the user/ISS. We have established that the Andor iXon X3 897 EMCCD can satisfy the derived requirements for a 40 Hz closed-loop bandwidth with a custom CCD clocking scheme using a 32×32 pixel sub-frame read out at 1 kHz frame rate. This sub-frame size will be sufficient, under worst-case conditions, to allow tip-tilt correction using an off-axis reference star for at least 300 seconds, before a brief (< 1 second) interruption to fast tip-tilt mode is needed to reposition the sub-frame.

2.1 Optical design and layout

The FTT/NAS optical train is depicted in the left panel of Figure 1. Its essential features can be summarised as follows:

- Interception of the 95 mm diameter collimated output beam of the telescope with a large dichroic splitter. This diverts the "bluer' light to the FTT/NAS and allows the "redder" wavelengths to be transmitted to the beam combining laboratory;

- Focusing of the collimated beam using a large diameter apochromatic lens. For this application we have traded-off the slight chromaticity of a lens-based solution with the much more demanding angular stability ($\times 20$) and installation tolerance ($\times 9$) needed for a non-chromatic off-axis parabola;
- Folding of the converging beam path using two plane mirrors;
- Optimisation of the geometry of the folded path so as to keep the four principal optical components as close together as possible — these are all co-located on a single stiff baseplate — and so as to locate this baseplate and the sensor head and enclosure as far away from the table edge as possible.

The selection of this layout was mainly determined by practical constraints on the space available on the optical table. These constraints included presence of additional systems (shown in the right panel of Figure 1), limited clearance above the table, and a shallow angle of incidence on the dichroic mirror to allow its coating to be optimised for measuring fringe data on polarised targets in total intensity.

We have chosen a custom 1.525 m focal length triplet lens to use as the focusing optic in the FTT/NAS. This will comprise three cemented elements made of common, easily worked glasses (N-BAK4, N-KZFS4, and N-LAF2). These have been chosen so as to give excellent achromatic performance from 400 nm to 900 nm and a temperature-dependent focal length that will largely compensate for any thermal expansion/contraction of the steel top of the Nasmyth optical table. Only inter-seasonal focal changes will be necessary (for example by utilising fixed exchangeable spacers in positioning the camera mount).

2.2 Opto-mechanical design

The FTT-NAS opto-mechanical system will comprise two main assemblies; (i) a common baseplate assembly and (ii) the EMCCD camera and its thermal enclosure assembly. The layout of the two assemblies is shown in the right panel of Figure 1. Our design exploits the use of a single baseplate upon which the dichroic mirror, the focusing optic, and the two fold mirrors will be co-mounted. The baseplate will mitigate, to first order, the effects of any local differential tilts or deformations in the Nasmyth table induced during the night due to changes in temperature. Such local disturbances would lead to differential movements and angular shifts of the FTT/NAS optical components. The EMCCD camera will be mounted on its own baseplate which covers a significant area of the Nasmyth table so as to similarly reduce the effects of local deformations of the table surface.

The common baseplate (including the optics mounts) and the EMCCD camera mount will be made of identical aluminium alloy and will both employ kinematic seat arrangements to allow for differential expansion of the baseplates and the steel of the optical table. The mounting components and materials of both assemblies will be matched to ensure that the centre of the focusing optic and the EMCCD camera move together as the temperature changes. As part of this strategy, the lens mount utilises "material compensation" to accommodate the difference in thermal expansion coefficient between the glass lens and its aluminium mount — the lens support pins being made of a high-expansion polymer and fabricated to a precise length so that the lens remains centred in the mount as the temperature changes.

This common baseplate approach also allows all the optical components to be positioned accurately relative to each other so that the installation inaccuracies will be determined only by machining tolerances. These have been kept well within the allowed image quality misalignment budget.

2.3 Thermal design

The vendor-specified minimum guaranteed operating temperature for the FTT/NAS camera is 0 °C in a non-condensing environment and its minimum survival temperature is -25 °C. Therefore for operational and camera safety reasons the FTT/NAS camera will be located within an enclosure in which the air will be maintained close to ambient temperature but in any case not less than 0 °C. To prevent overheating of the camera, and to keep the surface temperatures near the optical beam within the required 2 °C of ambient, the camera enclosure will be insulated and heat removed from it.

The cooling loop intended for the electronics cabinets in the UT enclosure will be used to remove heat from the FTT camera thermal enclosure. This solution has the distinct advantage that the fluid that passes through the cold plates and then through the camera to remove the Peltier heat should never fall below 0 °C in normal operation. Consequently, there will be no need for a variable coolant flow through the camera enclosure. The

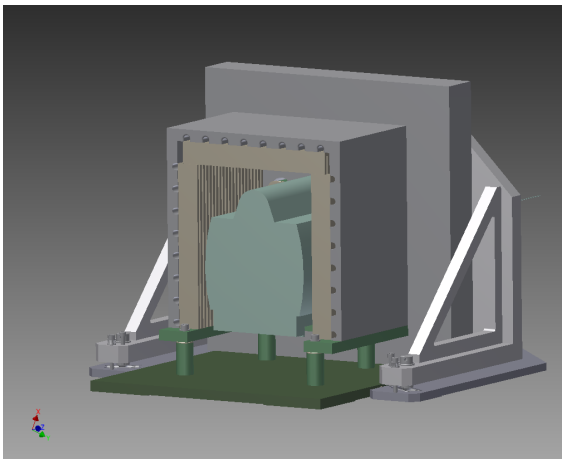

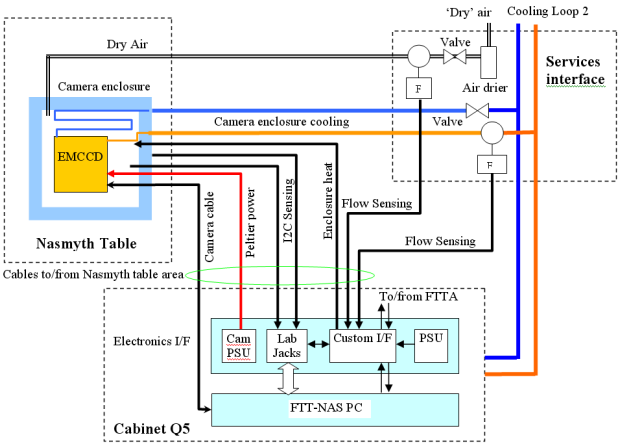

Figure 2. Left: View of the FTT/NAS camera enclosure with the insulation panels removed. The overall size of the enclosure is 340 mm tall by 340 mm wide and 320 mm deep and has insulation panel thickness of 50 mm. The camera is surrounded on three sides by finned cold plates which are connected in series with the camera Peltier cooling connections. The loops of the cold pipes running through the cold plates are shown in section. Right: The FTT/NAS camera environmental control and monitoring scheme showing the connections between the camera enclosure located on the Nasmyth table, the services interface panel located close by, and the electronics interface located with the FTT/NAS PC in the telescope enclosure cabinet. Connections to/from the tip-tilt mirror controller, located in the same electronics cabinet, are shown passing through the custom interface.

desired flow will be set by a manually adjusted valve and monitored by a flow meter for safety and setting purposes.

The enclosure will be constructed from rigid polyisocyanurate thermal insulation panels bonded to the outside of an aluminium frame formed from the cold plates used to remove heat from the enclosure. The outer surface of the insulation panels will be covered with a protective skin and the whole assembly will be supported from the optical table by low thermal conductivity spacers attached to the cold plate framework.

The cold plates are purpose designed and built so that the number of fluid connections within the enclosure is minimised. Each plate will be machined with straight channels to receive a nylon cooling tube that passes through all of the cold plates in a single continuous run. Heat-sinks will be connected to the plates to hold the tubing in place and force a good thermal connection to the cold plate.

As can be seen in Figure 2, the cold-plate assembly will be mounted on a frame supported by four pillars bonded to a baseplate which is clamped to the table top. The frame, pillars and baseplate will be made from a special low thermal conductivity glass fibre composite and provide an effective thermal break.

The camera will be located inside the enclosure on a mounting plate supported by pillars of low thermal conductivity glass fibre composite that pass through the insulation to the camera mounting bracket outside. A tube fixed to the camera mounting plate will also pass through the insulation and on through a hole in the camera mount. A window will be mounted so that air within the camera enclosure is prevented from escaping. The camera will be fixed only to the camera mount and will not be in contact with the independently-supported enclosure.

A dry air supply will be connected to the enclosure to ensure that humidity levels are low. Thermal sensors will monitor the cold plate and enclosure air temperatures and a humidity sensor will sense the enclosure air. A small heating element will be mounted in the enclosure so that the internal temperature can be increased if it is too cold for the camera to be operated.

2.4 Electronics design

The electronics for the FFT/NAS is located in an electronics cabinet within the telescope enclosure. The cabinet contains a rack-mount PC, which hosts the PCI cards for interfacing with the EMCCD camera and the Fast Tip-Tilt Actuator (FTTA) controller, and the following electronics and modules:

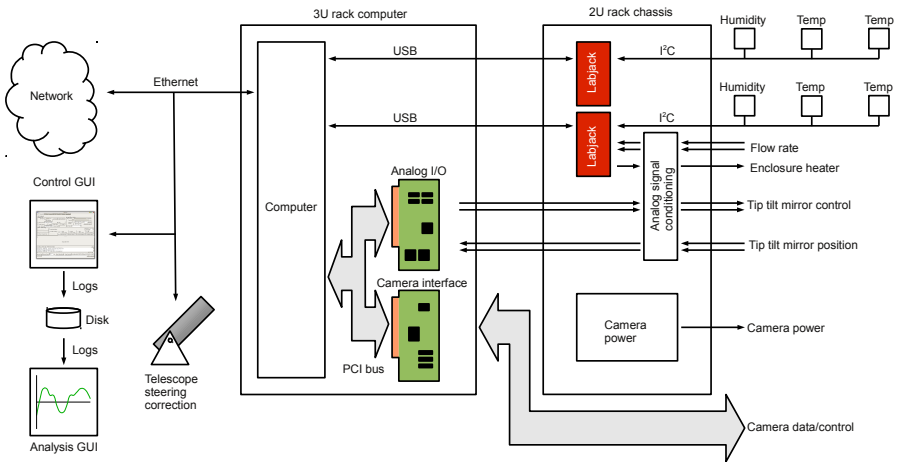

Figure 3. The proposed software execution environment for the FTT/NAS, showing the rack-mount PC, the hardware devices interfaced to it, and network connections to external software components.

- The EMCCD Peltier power supply module;
- Two Labjack analogue/digital I/O modules;
- A custom electronics interface circuit board;
- A power supply for the custom electronics.

The electronics design is concerned mostly with interfacing the signals between the FTT/NAS PC and the FTTA servo controller but also with providing analogue inputs for the various sensors that are necessary to monitor the camera thermal enclosure and the services provided to it. A diagram of how the FTT/NAS electronics in the cabinet are interconnected with the camera and its services is shown in the right panel of Figure 2.

For sensing and control low bandwidth interfacing will be handled using two of the computer's USB ports. Each port will connect with a Labjack U3 to provide access to an I^2C bus and a variety of digital and analog input and output connections. One bus will handle a humidity sensor and three temperature sensors associated with the camera thermal enclosure and the other bus will handle sensors placed outside the enclosure and on the Nasmyth table. The analog inputs available on the Labjack modules will connect via signal conditioning electronics on the custom circuit board to flow rate sensors used for monitoring the camera thermal enclosure coolant and dry air supplies. An analog output will control the camera thermal enclosure heater via an amplifier mounted on the custom circuit board.

2.5 Software design

The software execution environment for the FTT/NAS is illustrated in Figure 3. The system software will run on a rack mounted Intel-style computer. The operating system is expected to be Linux 2.6.32 with Xenomai 2.6 kernel patches, but the source code is compatible with more recent releases, including the forthcoming Xenomai 3.

Besides the interfaces to the FTTA controller and environment sensors described above, the computer will have a Gigabit Ethernet connection to the MROI control room via a local switch. This Ethernet link will be the conduit for the interface with the Interferometer Supervisory System (ISS) and operator GUIs.

2.5.1 Software architecture

The FTT/NAS software consists of two components used to control the FTT/NAS hardware, a user interface software application, and a fourth component used for offline visualization and analysis of previously-recorded monitor data.

The control software is partitioned into two components because of the need to maintain the environmental conditions within the FTT/NAS camera enclosure at all times, not just when the system is operational. The component responsible for controlling the camera environment and enabling/disabling the camera is called the "environment controller", and the component that performs the primary FTT/NAS functions such as target acquisition and fast tip-tilt correction is called the "system controller".

The environment controller will normally run continuously. The system controller runs when the interferometer is observing or preparing to observe. The system controller subscribes to monitor data from the environment controller in order to detect whether the environment controller has given it permission to operate the camera. In all other respects, the two systems function independently.

The control/display GUI provides a graphical user interface for commanding the system and environment controllers and for live display of their monitor data (including camera images). It can also record monitor data to a set of FITS-format files when requested to do so by the operator. The control/display GUI may be used in one of two modes: a "standalone" mode in which it is fully functional, and a "display-only" mode which can safely be used when the FTT/NA system is under the control of the central ISS.

The analysis GUI is used to visualize and process monitor data previously recorded to FITS files by the control/display GUI. It provides a general diagnostic capability by means of functions for displaying image sequences, graphing scalar monitor data, and simple data analysis.

The design of all components of the FTT/NAS software is essentially complete. At the time of writing (June 2012), preliminary versions of the system controller and control/display GUI have been written and are undergoing testing. A precursor to the environment controller is complete and has been used extensively for our opto-mechanical stability tests. Aspects of the analysis GUI have been successfully prototyped.

2.5.2 Software design and implementation

The operating system is Xenomai (`http://www.xenomai.org/`). It has two important properties that are exploited in this project:

- It runs in "hard real time". Consequently it reacts to hardware inputs and controls hardware outputs with minimal and predictable delays. This is a very useful property for introducing a computational element to servo loops, as is needed in the FTT/NAS.
- It coexists with Linux. This means that the richness of the Linux system infrastructure is available to the software whenever hard real time performance is not required.

Both Linux and Xenomai have a "user-space" and a "kernel space" component:

- Kernel space contains the core system functionality, such as hardware interfaces and memory management. Code running in kernel space has few restrictions on what it can do.
- User space is where the user interacts with the system. There are more restrictions on what code is allowed to do in user space, but it is much harder for user space code to crash the system.
- An interface is provided to allow applications to communicate across the barrier between user space and kernel space.

The system controller in particular makes extensive use of the user space and kernel space domains of both Xenomai and Linux. Further details of the design of the system controller and the other FTT/NAS software components are given immediately below.

System controller The system controller software performs acquisition functions, fast tip-tilt servo loop closure and transmission of system diagnostic information (including camera images) over the network. This software can be broadly divided into two parts:

- Code that implements the real time fast tip-tilt servo loop using Xenomai. This is implemented as one kernel space thread and one user space thread.
- Code that implements supporting functionality, including network control and monitoring, using several non-real-time threads in Linux.

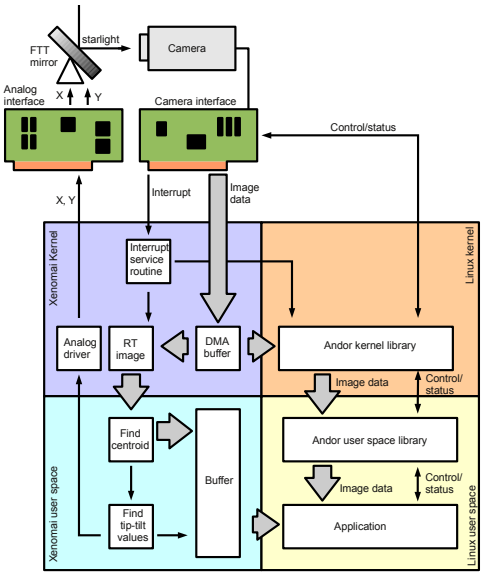

Figure 4. The implementation of the core servo loop in Xenomai and its connection with non-real-time Linux code.

The core function of the software is closure of the servo loop between the EMCCD camera and the fast tip-tilt mirror. This must be implemented within a hard real time operating system in order to guarantee calculations meet deadlines on every servo cycle. Xenomai is used because it is free, open source, well integrated with Linux, and proven during development of the MROI delay line metrology system.

The core software reads a camera image, calculates a centroid and then a correction, and sends the correction to the controller for the mirror. All this occurs in real time context. An interface is also provided to the remainder of the fast tip-tilt software, which runs in Linux. The implementation is illustrated in Figure 4.

When the camera interface card reads out a camera image, it writes the data to computer memory using direct memory access (DMA) and then triggers an interrupt to notify the computer that the transfer is complete. This interrupt is intercepted by an interrupt service routine that has been ported to Xenomai from Andor's open source driver, thereby providing real time access to image data while maintaining compatibility with the remainder of Andor's code. The interrupt service routine copies the image data to a buffer and blocks a Xenomai user-space routine from reading the data until the copy is complete.

When the user-space routine is allowed to read the data, it does so immediately. It firstly reads the computer's NTP stabilised system clock to timestamp the data[†], then it calculates image centroid coordinates, exploiting Xenomai's ability to use the computer's floating point hardware in real time context in user space.

A position error is then calculated from the centroid, which is used as the error input for the fast tip-tilt servo. An appropriate correction is sent to a custom Xenomai driver for the analogue interface card, which applies scaled voltages to the FTTA controller inputs.

Prototype centroiding and servo algorithms have been tested in a simulation environment, and the results of these simulations suggest that a system with our estimated optical throughput (86% from dichroic to camera) and the effective read noise we have measured for the Andor iXon X3, can meet the 16th magnitude limiting sensitivity requirement in the specified $0.7''$ seeing with an appropriate choice of closed-loop bandwidth.

Meanwhile the image data and corrections are buffered into an ordinary Linux application, where they are used for non-real-time tasks and logging. This buffering serves as an interface between the Xenomai code, which must meet strict deadlines, and the Linux code, which only needs to be able to keep up "on average".

[†]Xenomai V2.6 or later is needed to read the system clock in real time context and hence provide an accurate timestamp.

In addition to closing the fast tip-tilt servo loop, the system controller software must also set up and initiate readout of the camera, send tracking offloads to the unit telescope, execute commands and produce monitor data.

Two communications interfaces are provided for monitoring and control. These are the Generic System Interface (GSI)[3] used for communication with the ISS and an interface with the control/display GUI based on messaging protocols ("dlmsg") developed in Cambridge for the MROI delay line control software.[4] The system controller will only accept commands that change the system state from one source, currently set via a flag at compile time.

Environment controller The environment controller operates independently from the system controller so that it can function even when the camera is not in use. It is a simple sensing application which reads and reacts to data on timescales of the order of one second. Hence the environment controller has no hard real time requirements and runs in ordinary Linux. Interfaces with the ISS and control/display GUI are provided in the same fashion as for the system controller.

The application communicates with sensors and a heater via two USB-driven Labjack U3 boards. The sensors are either analogue voltage or I^2C types. The two Labjacks provide two independent I^2C buses, which will be helpful if two I^2C devices are needed that have the same I^2C address.

Control/display GUI The control/display GUI is a software application that provides an operator interface to the system controller and environment controller. The application is written in C and uses the GTK+ widget library. Images and scalar monitor data published by the systems are displayed to the operator, and these displays update automatically as new data arrive. The application can record the images and scalar data to a set of FITS files when requested to do so by the operator. The resulting files can be read by the separate offline analysis GUI. If the system and environment controllers are not being directed by an ISS supervisor, the control/display GUI is also used to control the FTT system.

Analysis GUI The analysis GUI provides access to the FITS log files that can be generated by the user of the control/display GUI. The application can be used to assess the images captured by the EMCCD camera during a particular recording or in plotting and analysis of guiding corrections. Other uses include:

- The review and plotting of seeing conditions;
- The examination of image profile;
- The measurement of image scales and distances between objects in the field of view;
- The review of the FTT/FLC system parameters.

The GUI is run under the Matlab environment. The main GUI deals with the selection and importing of FITS files or groups of recordings. Secondary windows may be spawned to provide additional analysis functionality.

3. LABORATORY TESTS

The principal aspects of the FTT/NAS that have been tested experimentally to date are those related to camera performance, i.e. latency and functionality of readout, and opto-mechanical stability. Preliminary tests of the thermal performance of the camera enclosure are now complete (as of June 2012), and will be followed by functional and performance tests of tip-tilt correction in closed-loop. The following sub-sections outline the relevant requirements, test procedures and results obtained thus far.

3.1 Camera readout testing

As mentioned in Sec. 2 tests have already been undertaken with an initial 23×23 pixel sub-array custom readout provided by the EMCCD vendor. The results confirmed that the frame rate and latency requirements for the FTT/NAS could be met with this small sub-frame with the camera operating at high gain and with an effective readout noise of $\sim 0.25 e^-$.

Element	Degree of freedom	Allocation to global stability budget
Dichroic	$\delta\theta_x$	$0.047''$
	$\delta\theta_y$	$0.045''$
Focusing optic	δx	0.47 µm
	δy	0.35 µm
	δz	140 µm
	$\delta\theta_x$	$0.75''$
	$\delta\theta_y$	$0.70''$
Fold mirror # 1	δz	0.59 µm
	$\delta\theta_x$	$0.090''$
	$\delta\theta_y$	$0.049''$
Fold mirror # 2	δz	0.31 µm
	$\delta\theta_x$	$0.064''$
	$\delta\theta_y$	$0.074''$
Camera mount	δx	0.47 µm
	δy	0.35 µm
	δz	140 µm
	$\delta\theta_z$	$2.32''$

Table 1. The stability budget allocations for the selected optical layout for the FTT/NAS. In each case the optic must not move by more than this amount for a 5 °C change in temperature. The co-ordinate system used has the z-direction normal to the named optical component, and the x- and y-directions perpendicular to this. In all cases, the x-direction is perpendicular to the surface of the Nasmyth optical table, and the figures represent "displacements" with respect to the symmetric expansion of the whole opto-mechanical layout.

Since then Andor have been customising a larger (32×32 pixel) sub-array fast-readout mode for us, and they have confirmed that a 1 kHz frame rate is achievable, with approximately 1 ms latency between readout and pixel data arriving in RAM. This rough measurement is consistent with a model of the camera readout that we constructed in order to explain our own timing measurements of the preliminary 23×23 pixel mode.

We have also measured the delay introduced by the real-time software in responding to the interrupt generated by the Andor PCI card, and calculating and outputting a correction signal. For a dual core 3 GHz AMD Athlon II computer, over many trials the maximum delay was measured to be 38 µs.

Putting these data together, we estimate that the latest 32×32 pixel mode will deliver a closed loop bandwidth of just over 43 Hz.

3.2 Opto-mechanical testing

Our opto-mechanical testing is described in more detail below. The first stage of our testing focused on assessing to what extent our proposed optical component mounts were able to meet the stability requirements needed for the FTT/NAS in the presence of the temperature changes expected at the Magdalena Ridge. More recently we have been testing the overall optical stability of the full optical system in a so-called "integrated test". This latter testing is not fully complete and so only preliminary results are presented here.

Table 1 shows the error budget for the maximum allowable component displacements that meet the top-level zero-point stability budget for our proposed optical layout. These displacements are relative to the tip-tilt zero point (guiding centre) determined at the start of night by projecting an alignment source onto the FTT/NAS camera from the beam combining laboratory.

3.2.1 Individual component testing

In order to test the thermal stability of the individual FTT/NAS component mounts, a thermal enclosure was constructed within which each of the mounts (with the relevant optic attached) could be introduced. The chamber was constructed of six cold plates, placed in pairs on the top and two side faces, which in conjunction with an aluminium baseplate made up a short tubular shell. The cold plates were supplied with temperature-controlled water from a Grant RC350G chiller, which was placed in an adjacent laboratory, and could be used to either

warm up or cool down the chamber. The fluid temperature could be controlled to roughly one degree Celsius, which proved more than adequate for our tests.

By cycling the water temperature according to a pre-determined schedule, the optical component mounts could be subjected to "environmental" temperature changes mimicking those that might occur during an observing night. This method of testing, however, is likely to have introduced errors associated with non-uniform cooling/warming of the mounts due to the forced air circulation in the chamber (small fans were used) and possible uneven mixing of air in the chamber. These inaccuracies are most likely to have occurred at the start of each cooling cycle, as aggressive cooling of the chamber was taking place.

The optical mounts were typically set up within the chamber with position sensors attached such that any relative motion between the mount and the optic could be determined. In addition, further sensors were used to monitor, for example, the chamber temperature, the temperatures of different parts of each mount and the ambient temperature outside the chamber.

The position sensors used were Linear Variable Displacement Transducers (LVDTs) which were typically able to measure displacements as small as 50 nm. Because LVDTs themselves exhibit a temperature-dependent response, in all cases the measurements obtained with them were calibrated against known temperature-dependent motions (for example the expansion of a solid aluminium alloy block) measured with identical sensor/mounting arrangements.

Mirror piston tests A typical set of test results associated with the piston stability of the dichroic/fold mirror mounts, i.e. the extent to which changes in temperature give rise to motion along the beam propagation (z-) direction, is presented in Figure 5. This shows the uncalibrated z-motion of a fused silica mirror as a function of chamber temperature, in this case changing from roughly 13 °C to 23 °C, together with the uncalibrated measurement of a reference block. Also shown is the difference in these two measurements: this represents the actual calibrated piston motion of the optic. This is very stable with temperature, with only small variations of at most 100 nm peak-to-peak. This can be compared with a piston stability requirement of roughly half a micron, i.e. a factor of five larger, and confirms that the mounts are behaving as designed, easily meeting the FTT/NAS piston stability requirement.

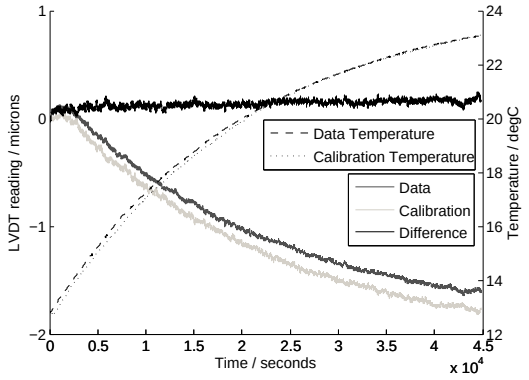

Figure 5. Raw (light and mid grey) and calibrated (black) piston fluctuations measured in a typical dichroic/fold-mirror piston test. There is a small (quarter of a degree) difference in the temperature profile for the measurement and calibration experiments, with the temperature in the test chamber rising from roughly 13 °C to 23 °C in each case. Note that the raw uncalibrated measurements only show a variation that is a factor of a few greater than the allowed piston fluctuations, and the calibrated measurements are a factor of five smaller than the requirement.

Mirror tilt tests A typical set of test results associated with the tilt stability of the dichroic/fold mirror mounts is presented in Figure 6. In this case the left hand panel shows the uncalibrated LVDT data in light grey, the LVDT calibration data in mid grey, and the difference of these two, representing the actual tilt, in

black. The graph has been scaled such that a linear displacement of 0.045 microns corresponds to the stability requirement for the dichroic mirror mount (i.e. 45 milliarcseconds).

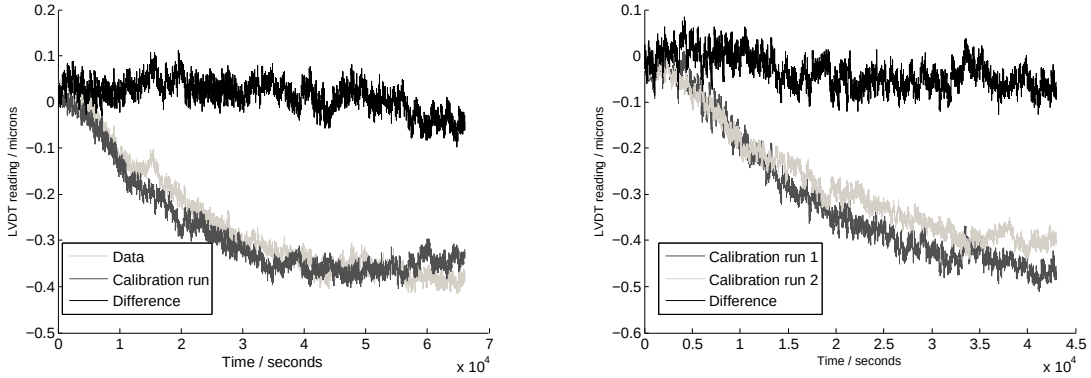

Figure 6. Left: measured (light and mid grey curves) and calibrated (black curve) LVDT tilt data expressed in microns for a dichroic/fold-mirror mount test. The allowed tilt variation expressed in these units for the temperature change here is 45 nm. Right: equivalent data for two calibration runs. In this case the recovered signal is expected to be zero. The level of residual fluctuations in the black trace is indicative of the level below which calibration errors cannot be eliminated. Overall, these data suggest that the prototype mount may be compliant with its tilt stability requirement, but if it is not, it is unlikely to have exceeded it by more than a factor of two.

The data appear to show a slowly decreasing trend with temperature (this is again rising by roughly 10 °C over the course of the ten-hour measurement time) of about 0.075 microns, roughly 70% greater than the FTT/NAS budget allows. In order to assess the reliability of this result, additional experiments were run where calibration data from a given experiment were calibrated using measurements from a calibration made on a different day. One such "cross-calibrated" dataset is shown in the right-hand panel of Figure 6. These data suggest that our test set-up is limited by calibration uncertainties to a level of no better than twice the angular shift allowed by the optical stability error budget.

In summary, our experimental data demonstrate that the dichroic/fold mirror mounts may satisfy the tilt stability budget allocation, and are very unlikely to have exceeded it by more than a factor of two.

Lens shear tests The tolerances on the tilt and piston stability of the FTT/NAS lens mount are factors of 10–100 times greater than for the dichroic/fold-mirror mounts, and so given that they share a common design approach, tests of these aspects of the lens mount stability have not been prioritised. Rather, it is the required half-micron stability (for $\Delta T = 5$ °C) in x- and y-position of the lens, perpendicular to the direction of beam propagation, that is likely to present the greatest design challenge.

Our test for this motion utilised a pair of LVDT probes mounted along a diameter of the lens and monitoring the centration of the lens within its aluminium mount while the chamber temperature was changed (see left panel of Figure 7). The right panel of Figure 7 shows the results for a lens shear test where the lens support pins were deliberately fabricated with an incorrect length. Similar tests using other pairs of incorrectly fabricated pins allowed us to determine the correct length needed to give no lens shear as 16.1 ± 0.8 mm. Quite separately we measured the CTE of the pins in a laboratory test set-up. These, and other repeat data, were then used to independently compute the pin length needed to keep the lens centred. This gave a value of 16.5 ± 0.9 mm, consistent with the LVDT predictions, and confirming that our material compensation strategy can meet the FTT/NAS requirements.

A summary of the results of our component mount tests is presented in Table 2.

[‡]In the case of lens shear, the value listed is the movement predicted assuming a 1 mm error in the compensating pin length based on the movements seen with pins of other lengths.

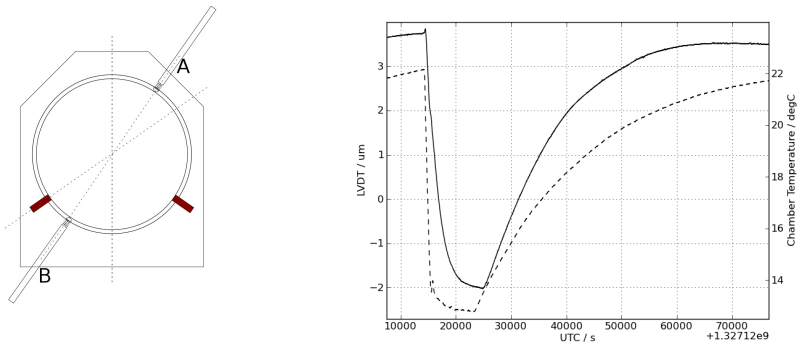

Figure 7. Left: A face-on view of the triplet lens mount showing the LVDT measurement probes in place and the polymer pins that support the lens in the radial direction. Right: FTT/NAS Lens shear (solid line) and chamber temperature (dashed) as a function of time during a thermal cycle test. In this example, the polymer pins supporting the lens were deliberately fabricated with the incorrect length and so the lens does not remain centred in its mount but moves by roughly 1 µm/°C.

Element	Degree of freedom	Measured motion	Required stability	Comments
Dichroic/mirror mount	Piston stability	100 nm	< 500 nm	Compliant
Dichroic/mirror mount	Tilt stability	≤ 100 nm	45 nm	Compliant within factor $\lesssim 2$
Lens mount	Shear stability	≤ 250 nm[‡]	~ 350 nm	Compliant

Table 2. Comparison of the FTT/NAS component stability test results and the performance needed to meet the top-level requirements. The dichroic/fold mirror mount tilt stability requirement has been converted into a linear measure.

.

3.2.2 Integrated testing

The focus of our most recent opto-mechanical testing has been to attempt to validate the full optical train of the FTT/NAS. To this end a much larger thermal chamber has been constructed which allows for the full optics baseplate, with optics, to be mounted on an optical table in our laboratory and then be temperature cycled. The interfaces between the baseplate and the optical table are identical in concept to those designed for the FTT/NAS but have been fabricated to a slightly lower level of precision.

The design of the chamber, depicted schematically in the left panel of Figure 8, and shown part assembled in the photograph in the right panel, allows for a 9 mm diameter collimated beam from a HeNe laser to be injected along the optical train and be measured on exit from the optical system via a small open port "3". This measurement is performed by a CCD camera mounted to the optical table externally and close to its boundary. Similarly, the input beam can also be measured after (i) passing through the dichroic at location "R"; (ii) passing through a semi-silvered fold mirror 1; or (iii) passing through a semi-silvered fold-mirror 2. The rationale for this approach is that, by simultaneously measuring the output beam and, for example, the beam exiting at port R, one can in principle remove the effects of any instabilities in the laser beam injection direction from motions seen in the output beam. Simultaneous measurement of the beams exiting at the other calibration ports may be used to assess other types of systematic errors and can help identify any unstable components.

The typical sequence for a test was that the chamber was held at room temperature for several hours, and then chilled to roughly 10 °C below ambient over three hours, during which time the output beam as well as one of the "calibration" output beams were monitored. Thereafter, the chamber temperature was allowed to return to the ambient level over a longer period.

A typical integrated test result is shown in Figure 9. This shows the "calibrated" exit beam motion — measured in camera pixels, where motions of up to 0.3 pixels are allowed — plotted as a function of time. The chamber temperature is shown by the dotted trace, and fell by roughly 4 °C over the course of the first three hours of the run. In these data the spot position variations have been corrected for both the observed motions

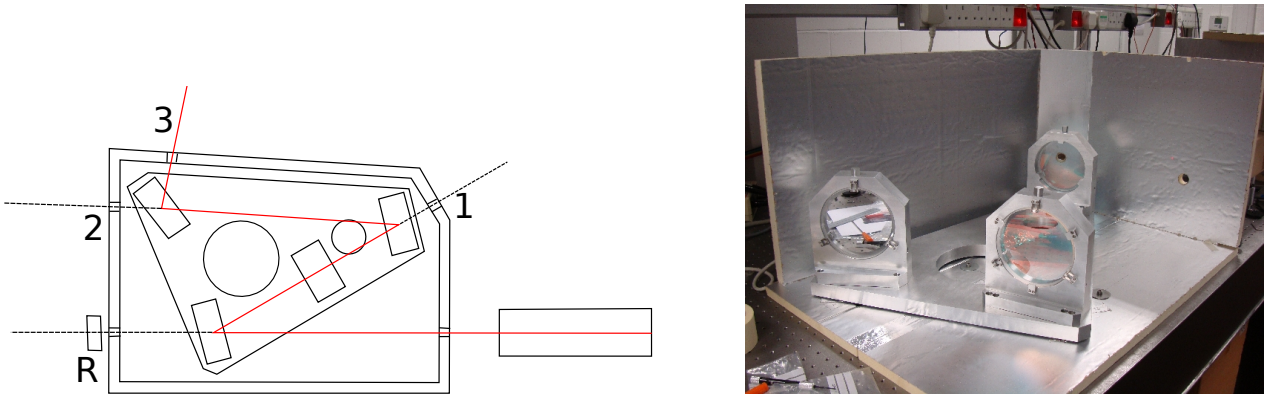

Figure 8. Left: The optical arrangement used for the FTT/NAS integrated test. A collimated laser beam enters from the right, part reflects off the dichroic (at bottom left), passes through the lens and then off the two semi-silvered fold mirrors before exiting at port 3. Ports R, 1 and 2 the beam to be interrogated after travelling successively longer portions of the optical train. Right: A view of the FTT/NAS optics mounted on their baseplate and enclosed by a partially assembled thermal chamber.

of a calibration beam exiting at port 1, and the shear in the vertical direction associated with the material compensation of the lens mount. This is because the camera and lens system being used to monitor the exit beam motion is not subject to the temperature changes experienced by the lens mount itself.

The most noticeable features of Figure 9 are the extreme motions of the exit beam direction at certain times during the experiment. Exhaustive tests have confirmed that these large amplitude motions are exclusively associated with abrupt changes in the temperature difference between the top and bottom skins of the optical table on which the tests are being undertaken. It appears that at key times during the experiments, notably (a) when the cooling cycle is initiated and (b) when active cooling of the chamber is stopped and the temperature of the thermal enclosure is allowed to increase slowly back to ambient, the optical table undergoes a thermal shock and the calibration measurements are compromised. These times are identified by the horizontal arrows in Figure 9 and last no more than an hour.

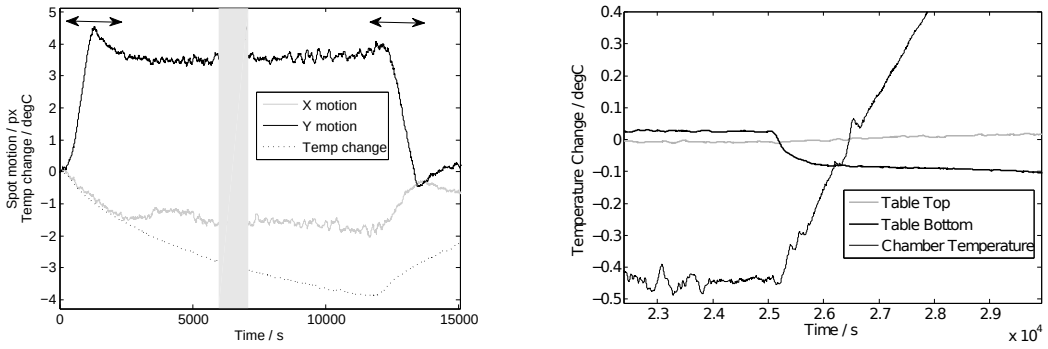

Figure 9. Left: Typical results from an FTT/NAS integrated test showing the "calibrated" motion in x- and y- for a laser beam that has propagated the full optical train. The grey band indicates times at which the data-logger failed. In this experiment the chamber temperature has been dropped by 4 °C and the corresponding allowed image motion is 0.3 pixels. The horizontal arrows show the times at which the largest excursions are seen, and during which the ΔT between the top and bottom skins of the optical table jumps rapidly. Outside these periods the observed beam motion is approximately at the level of twice the FTT/NAS requirement. Right: The measured temperature of the top and bottom skins of the optical table during a "warm-up". In these data the water chiller for the thermal chamber was adjusted (at t$\sim 25,000$ seconds) so as to allow the chamber to slowly rise to ambient conditions. Note the abrupt change in the lower skin temperature which is matched by a much more gradual increase in the upper skin temperature.

We conclude that our data have identified a warping of the top and bottom optical table surfaces, and resulting changes in the positional and angular orientation of the laser beam and the FTT/NAS baseplate (since the locations of its kinematic seats are altered). This effect is not fully compensated by our calibration strategy. We believe that there is also a contribution from warping of the baseplate due to a changing temperature differential between its upper and lower surfaces.

At other times in the course of the tests, when the differential skin temperature of the optical table is stable, *but importantly while the chamber temperature is changing by several degrees Celsius*, the calibrated spot motion is very stable. During these periods the observed motion is approximately at the level of only twice the FTT/NAS requirement. This is consistent with the results of our individual component mount tests, and indicative that we are very close to meeting the overall FTT/NAS zero-point stability requirement.

We are intending to continue our integrated tests, with the goals of monitoring any table surface motions directly, reducing any cooling-induced temperature shocking of the optical table, and improving the temperature equilibration of the common baseplate.

4. CONCLUSIONS

We have presented a comprehensive design for the FTT/NA system together with test results which allow us to predict the expected opto-mechanical stability and closed-loop bandwidth. There are ambiguities in interpreting the integrated test results we have obtained thus far, but we believe the results are consistent with the component test results which indicate that we will exceed the zero-point stability requirement by a factor of roughly 2. If left uncorrected, such zero-point drifts would have a small impact on the limiting sensitivity (equivalent to 6% throughput loss) and calibration accuracy of MROI. However we will correct these drifts using the continuous tilt/shear correction system that has now been incorporated into the MROI system design, and our measurements confirm that they are slow enough to be fully corrected.

Having passed a Preliminary Design Review in May 2012, the Cambridge team is proceeding with refinement and manufacture of our current design. Procurement and manufacture of the opto-mechanical components will be done in parallel with continued software development. These activities will come together in the setting up of a closed-loop laboratory demonstration that will correct artificially-generated fast tip-tilt perturbations. We expect to begin the closed-loop laboratory tests within a 6 month timescale, and subsequently to commence integration activites on the Magdalena Ridge during 2013.

ACKNOWLEDGMENTS

The Magdalena Ridge Observatory (MRO) interferometer is hosted by the New Mexico Institute of Mining and Technology (NMIMT) in Socorro, NM, USA, in collaboration with the University of Cambridge, UK. MRO is funded by Agreement No. N00173-01-2-C902 with the Naval Research Laboratory and an institutional revenue bond issued by NMIMT. We wish to also acknowledge funding for Cambridge University staff from STFC in the UK.

REFERENCES

[1] Creech-Eakman, M. J., Romero, V. D., Payne, I., Haniff, C. A., Buscher, D. F., Farris, A. R., Jurgenson, C. A., Santoro, F. G., Selina, R. J., and Young, J. S., "The Magdalena Ridge Observatory interferometer: a status update," *Proc. SPIE* **8445** (2012). Paper 8445-23, these proceedings.

[2] Buscher, D. F., Bakker, E. J., Coleman, T. A., Creech-Eakman, M. J., Haniff, C. A., Jurgenson, C. A., Klinglesmith, III, D. A., Parameswariah, C. B., and Young, J. S., "The Magdalena Ridge Observatory Interferometer: a high-sensitivity imaging array," *Proc. SPIE* **6307**, 11 (2006).

[3] Farris, A., Klinglesmith III, D. A., Seamons, J., Torres, N., Buscher, D. F., and Young, J. S., "Software architecture of the Magdalena Ridge Observatory Interferometer," *Proc. SPIE* **7740**, 77400R (2010).

[4] Young, J. S., Boysen, R. C., Buscher, D. F., Fisher, M., and Seneta, E. B., "Software and control for the Magdalena Ridge Observatory interferometer delay lines," *Proc. SPIE* **7013**, 70134C (2008).